Iraqi Journal of Biotechnology, 2025, Vol. 24, No. 2, 215-229

In Vitro Synergistic Effect of CaO Nanoparticles and Naringenin to Inhibit Multidrug-Resistant *Staphylococcus aureus* and Expression of *lukE/D* Genes

[1*]Iman A. Al-Essawi , [1]Mayada A. Shehan , [2]Mazin A. Alalousi

[1]University of Anbar/ College of Science / Department of Biology
[2]University of Anbar/ College of Science / Department of Physics

Received: April 1, 2025 / Accepted: May 6, 2025 / Published: July 5, 2025

Abstract: The need to investigate therapeutic alternatives has increased due to the rise in bacterial infections that are resistant to antibiotics. One promising direction is the synergy between natural materials and nanoparticles, which can benefit various fields, including medicine, agriculture, and environmental science. Combination therapy is particularly relevant in the context of antimicrobial CaO nanoparticles with Naringenin on multidrug-resistant *S. aureus.* The current study studied the effect of treatments on the expression of *luk/lukD* in isolates collected from different samples. All isolates were identified as *S. aureus* according to morphological, cultural, biochemical, VITEK-2, and *16S rRNA.* The study found that the isolates were resistant to Cefoxitin, Oxacillin, Erythromycin, Vancomycin, Clindamycin, Tetramycin, Levofloxacin, Moxifloxacin, Imipenem, and Meropenem. CaO nanoparticles were prepared from eggshells using the milling method followed by calcination at 900 (°C) and characterized by XRD, SEM, and TEM analysis. A qPCR assay was performed to evaluate the transcription level of *lukE* /*lukD* genes in *S. aureus*. The results showed a synergistic effect of CaO nanoparticles with Naringenin on multiresistant cocci.

Keywords: CaO nanoparticles (CaONPs), Naringenin (NAR), *LukE/D* genes, *Staphylococcus aureus.*

Corresponding author: (Email: ima22s1008@uoanbar.edu.iq).

Introduction

Staphylococcus aureus is a common cause of wounds, postoperative, prosthetic joint steps, and even fatal pneumonia infections. Treatment of *S. aureus* infections is difficult due to several virulence factors, antibiotic resistance, and no effective vaccine (1).

Toxins, immunomodulators, and adhesins are virulence factors that have various harmful roles in *S. aureus*. There has been continued interest in the unusually high number of toxins and other virulence factors produced by *S. aureus*, how they contribute to disease, and finding alternative and safer treatments (2).

Leukocidin ED is a type of pore-forming toxin. LukED toxin plays a prominent role in the pathogenesis of *S. aureus*. Where can destroy host cells by perforating their membranes, causing them to lyse (3). The toxin LukED was present in 87–93% of pathogenic strains from Japan and 88–99% of Methicillin-resistant *S. aureus* strains worldwide, indicating its possible role in the pathogenicity of *S. aureus* (4). *S. aureus* strains can produce up to five leukocidins that target and kill host

phagocytes (5). Drug-resistant *S. aureus* isolates that show elevated expression of genes encoding Leukocidin toxins (*lukE, D, F, S*) are often responsible for hospital infections (6). The rapid development of microbial resistance outpaces the creation of new antibacterial agents, highlighting the urgent need for effective alternatives. In this context, metal nanoparticles and metal oxides emerge as promising candidates in the battle against antimicrobial resistance. (7). Additionally, combination therapy is an under-explored strategy that holds the potential for addressing AMR more effectively. This approach could offer a viable solution to the growing resistance challenge (8). Targeting bacterial cell membrane lipids and virulence factors such as bacterial toxins, represent a novel alternative to conventional antibiotic therapies. This approach can enhance antibiotic susceptibility by altering the bacterial membrane's composition and affecting properties such as stability, permeability, fluidity, and surface charge(9).

Nanomaterials are materials with external dimensions of one nanometer. Several manufacturing processes create these materiales. They are used in the pharmaceutical industry, which is the most important industry Shape, size, surface morphology, crystallinity, solubility, affect the physical and chemical properties of these nanostructures (10). The rise in bacterial infections and their multidrug-resistant properties are driving the development of a new class of antimicrobial agents, including the use of metallic nanoparticles in novel formulations (11).

There is a lot of promise for using CaONPs as antibacterial agents in the food industry (12). CaONPs are beneficial in catalysis, and adsorption. CaONPs are also applicable against *Escherichia coli*, *Streptococcus mutans*, and *Proteus vulgari* (13). CaONPs with salicylic acid enhance the effectiveness of plant defenses against *Fusarium oxysporum* by increasing the production of antimicrobial peptides, which increases the production of resistance to this fungus (14). CaO nanoparticles (CaONPs) prepared using 600 mJ laser energy showed high resistance against *S. aureus* and *Klebsiella pneumoniae* (15). CaONPs with Graphene oxide reduced the expression of water stress-related genes (*mtr-miR159* and *mtr-miR393*) in alfalfa (16).

Naringenin (NAR) is a compound trihydroxy flavanone found in citrus fruits and some plants, known for its many health benefits, like fighting cancer and infections (17). Naringenin provides protection against oxidative stress, enhances the ability of cells to fight damage caused by free radicals, and reduces toxicity caused by substances such as paraquat. Thus, it promotes cell health(18). Modifying their chemical structures can significantly impact their solubility, stability, and biological activity. It reduces harmful biofilm formation and works well with antibiotics like oxacillin, enhancing their effectiveness. This makes it a potential candidate for treating resistant infections (19). Novel Naringenin derivatives showed varying levels of antimicrobial activity, with some substitutions enhancing effectiveness while others reduced it. Naringenin's ability to kill bacteria is linked to damaging the protective membrane and interfering with the DNA.

This dual action makes it a powerful antibacterial agent (20). NAR helps

colistin fight bacteria more effectively by blocking resistance, confusing the bacteria's defense systems, and increasing damage to the bacteria (21). NAR shows clear effects on gut bacteria, which in turn improve microbiome health and increase the expression of iron uptake genes in *Ruminococcus gauvreauii*. In *Bifidobacterium catenulatum*, increased expression of metabolic and DNA repair genes was observed, with a decrease in thymidine synthesis genes. *Enterococcus caccae* showed increased expression of transcription and protein transport pathways, with a decrease in sugar transport and purine synthesis genes (22). The present study aimed to investigate the synergistic effect of CaONPs with NAR to inhibit the growth of *S. aureus* and the expression of leukocidin toxin genes in this bacterium. The study is assuming that the synergistic effect of CaONPs with NAR gave good inhibition results and reduced the expression of toxin genes more than using each substance alone, which is encouraging for future work as an antimicrobial agent.

Materials and Methods

Isolation of *Staphylococcus aureus*

Staphylococcus aureus was isolated from 160 samples with Mannitol salt agar plates for 24 hr. They were picked out and identified as *S. aureus*, based on their morphological and biochemical characteristics, VITEK-2 compact system (Biomerieux, France), and Detection of *16SrRNA* FW GGGACCCGCACAAGCGGTGG RW GGGTTGCGCTCGTTGCGGGA (191) bp (23)—conventional PCR. The primer was supplied in a lyophilized form by the Macrogen company (Korea).

Detection of *lukE* and *lukD* by conventional PCR

lukE and *lukD* conventional PCR primers were supplied by the Macrogen company (Korea). The primers of amplify the two genes are:
Fw TGCGTAAATACCAGTTCTAGGG, Rw TCCAACAGGTTCAGCAAGAG (199 bp) and
Fw ACCAGCATTTGAACTACTTTGT, Rw TCTAATGGCTTATCAGGTGGAT (240bp) respectively (24).

Antimicrobial Resistance (AMR) Test

A total of ten *Staphylococcus aureus* isolates were subjected to an antibiotic susceptibility test (AST) card in the Vitek2 compact system (Biomerieux, France). The isolates were tested for 10 different antimicrobials, namely, Cefoxitin, Oxacillin, Erythromycin, Vancomycin, Clindamycin, Tetramycin, Levofloxacin, Moxifloxacin, Imipenem, and Meropenem.

Synthesis of CaO nanoparticles (CaONPs)

The chicken eggshells were collected, cleaned thoroughly, ground, washed three times with deionized water to remove impurities, then ground into a fine powder using a blender. The resulting eggshell powder was roasted for 1 hour in a sealed vessel at 900 °C in a furnace oven (India), the powder was cooled (25). CaO powder was added to deionized water next, and an ultrasonic probe from Hilcher (Germany) was used for 15 minutes. Operating at a frequency of 20–30 kHz, this probe helps distribute calcium oxide particles evenly throughout the solution. The ultrasonic waves generate a cavitation effect, which breaks up the particles and prevents

agglomeration, enhancing the mixture's effectiveness and making it suitable for preparing nanofluids and improve its antibacterial properties (12).

Preparation of naringenin (NAR)

Naringenin (purity 97 %) was purchased from MACKLIN (China) for this study. In the disk diffusion assay. The solvent of choice for NAR was methanol(26). Serial dilutions (23 to 0.7 mg/ml).

Preparation of CaONPs-NAR

One mL of CaONPs (0.7mg/ml) was mixed with one mL (23mg/ml) of naringenin solution under stirring conditions at 30 °C. This resulted in the formation of a yellow substance.

Characterization of CaO nanoparticles (CaONPs)

Calcium oxide nanoparticles were characterized using several tests to determine some of their physical and chemical properties, such as XRD, SEM, and TEM (27,28).

The structural characteristics of the produced CaONPs were examined using an X-ray diffraction apparatus with a (°2Th) 0.0110 step size and a wavelength of 1.54060 as the powdered sample was applied to silicon wafer chips.

The surface of a sample can be captured in high-resolution images through scanning electron microscopy (SEM). This method is applied in many disciplines, such as materials science and biology. SEM directs a concentrated electron beam onto the sample's surface to produce finely detailed images with compositional and topographical details. Important information regarding their size, shape, and crystallinity can be obtained through transmission electron microscopy (TEM).

Effect of CaO nanoparticles (CaONPs) and Naringenin (NAR) on *Staphylococcus aureus* isolates and expression *lukE/D* genes

The effect of treatments (CaONPs, NAR, CaONPs-NAR) on *S. aureus* isolates was tested using the agar diffusion method. By mixing 0.007 g of CaONPs with 10 ml of deionized water (0.7 mg/mL), a CaONPs stock solution was prepared, and serial dilutions (1/2 (0.35), 1/4 (0.175), 1/8(0.0875), 1/16(0.043), and 0) were used by combining deionized water with a known amount of base solution. Dilutions of NAR were also made from 0.23 g of stock solution in 10 mL of methanol (23 mg/mL) (1/2 (11.5), 1/4(5.75), 1/8 (2.875), 1/16 (1.437), and 0) and a stock solution of CaONPs/NAR at the same concentrations. A suspension of bacteria was prepared and compared with a 0.5 McFarland tube. The bacterial suspension was spread on Mueller-Hinton agar plates. Prepared Petri dishes with wells of 10 mm diameter on agar plates. 100 µL of prepared CaONPs, Naringenin solution, and prepared solutions of CaONPs-NAR were loaded in different wells in the Mueller agar plates. The agar plates remained undisturbed for 15 min to ensure even diffusion of samples into the agar. The plates were incubated for 18-24 hours at 37˚C.

A qPCR test was carried out to evaluate the transcription level of the *lukE*, *lukD*, and *16SrRNA* as reference genes in *S. aureus*. A one-step RT-PCR kit was used that uses RNA as a template for replication. In this study, two primers were used to detect the effect of CaONPs and NAR on gene expression (29, 30). The percentage increase in fold for the

treatments was calculated as follows: Increase in fold % =(C)-(CD) /(C)×100. Whereas:
C: The mean of the change in the fold for the control
CD: The mean of the change in the fold for the treatment.

Statistical Analysis

Data from three replicates was used to calculate the mean and standard deviation. GraphPad Prism 10 software was used to plot graphs, and analysis of variance (ANOVA), followed by the Tukey test, was performed to determine statistically significant differences between treatments.

Results and Discussion

Detection and Identification of *S. aureus* isolates

Sixty of *S. aureus* isolates were obtained from several clinical sources. The isolates of *S. aureus* that grew on the mannitol salt agar after 24-48 hr. at 37°C (Figure 1) or blood agar media were subjected to microscopic, cultural, and biochemical analysis, VITEK-2, and *16SrRNA* (31,32). Figure (2) showed one band of 191 bp (product size) in the *S. aureus* isolates and the control as a result on agarose gel compared with DNA marker (100-1500 bp).

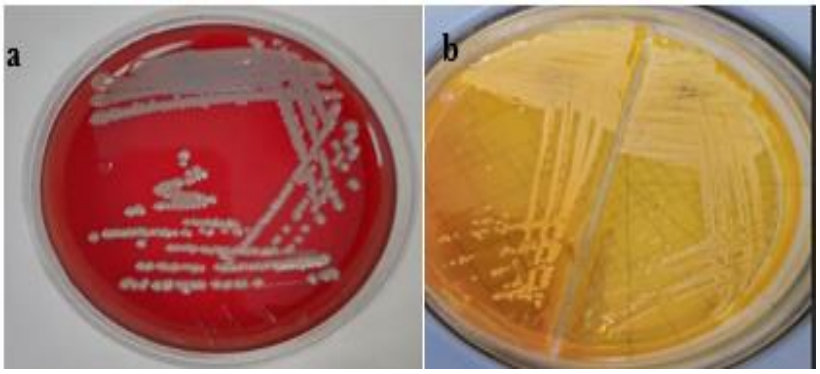

Figure (1): (a) *S. aureus* on Blood agar (b): Mannitol salt agar

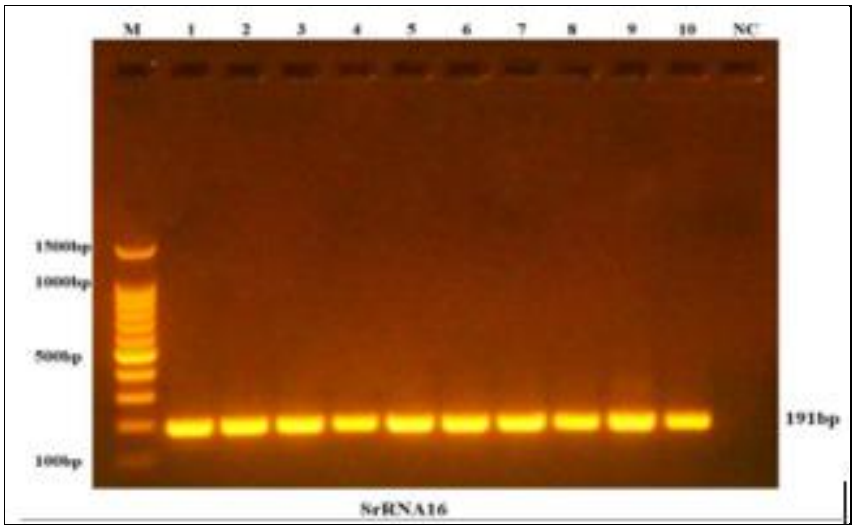

Figure (2): Results of the polymerase chain reaction (PCR) of *SrRNA16* genes in *S. aureus* isolates on 1.5% agarose gel electrophoresis stained with Ethidium Bromide, M: 100bp ladder marker. Lanes 10 resemble 191bp PCR products.

Detection of *lukE* and *lukD* in *S. aureus* isolates

The molecular investigation was carried out on ten isolates that carried *lukE*, and *lukD* genes that encode to Leukocidin ED toxin using the polymerase chain reaction PCR (33). The PCR products of the *lukE* (199bp), *lukD* (240bp) were confirmed using a gel electrophoresis system as shown in (Figures 3-a and 3-b).

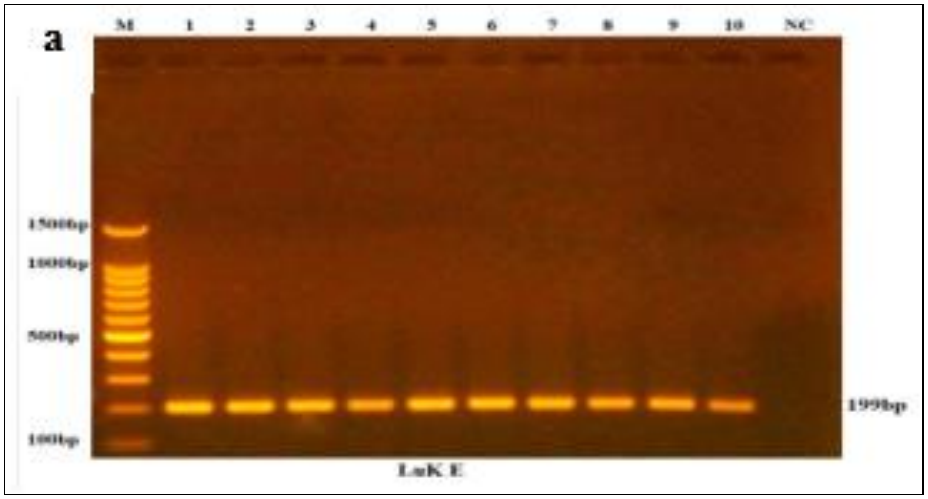

Figure (3-a): Results of amplifying *lukE* in *S. aureus* isolates on 1.5% agarose gel electrophoresis stained with Ethidium Bromide, M: 100bp ladder marker. Lanes 10 resemble 199bp PCR products.

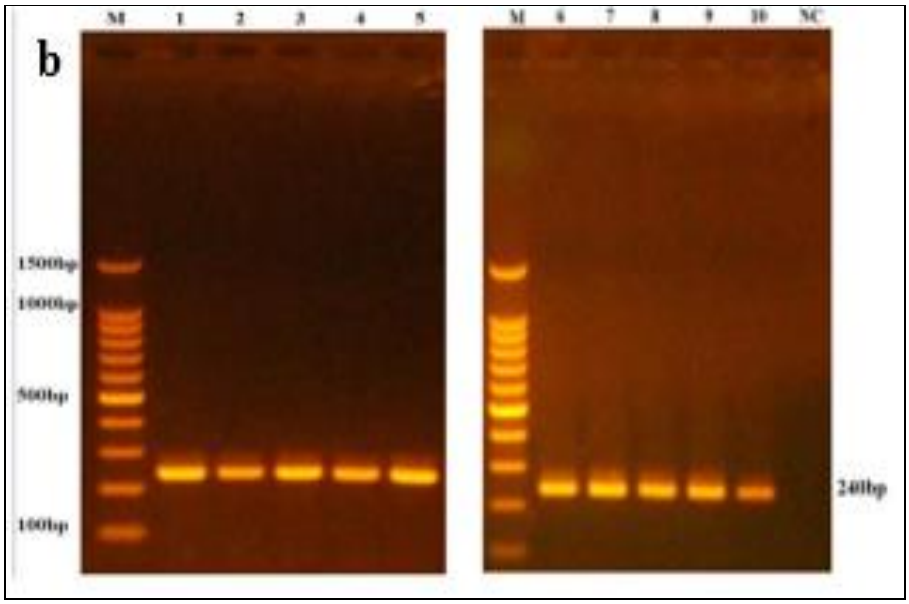

Figure (3-b): Results of the polymerase chain reaction of *lukD* in *S. aureus* isolates on 1.5% agarose gel electrophoresis stained with Ethidium Bromide, M: 100bp ladder marker. Lanes 10 resemble 240bp PCR products.

Antimicrobial Resistance (AMR) Test

Ten isolates were subjected to ten antimicrobial agents for antimicrobial resistance testing. The results of antimicrobial resistance testing showed that the ten *S. aureus* isolates were resistant to oxacillin and cefoxitin (100%) and showed different resistance

rates to eight antimicrobials (Table 1) isolates were found to be resistant to eight antimicrobials, namely Erythromycin 90%, Vancomycin 80%, Clindamycin70%, Tetracycline70%, Levofloxacin 70%, Moxifloxacin 70%, Imipenem 30%, Meropenem 30%.

Table (1): Resistance of *Staphylococcus aureus* isolates to 10 different antimicrobials.

Isolates number / Antibiotic	S1	S2	S3	S4	S5	S6	S7	S8	S9	S10	Resistance %
Cefoxitin	R	R	R	R	R	R	R	R	R	R	100
Oxacillin	R	R	R	R	R	R	R	R	R	R	100
Erythromycin	R	R	R	R	R	R	R	R	R	S	90
Vancomycin	S	R	R	S	R	R	R	R	R	R	80
Clindamycin	R	R	R	R	S	R	S	S	R	R	70
Tetracycline	R	R	R	R	S	R	R	S	R	S	70
Levofloxacin	R	R	R	R	R	R	S	R	S	S	70
Moxifloxacin	R	R	R	R	R	R	S	R	S	S	70
Imipenem	S	R	R	R	S	S	S	S	S	S	30
Meropenem	S	R	R	R	S	S	S	S	S	S	30

Characterization of CaO nanoparticales (CaONPs)

X-ray diffraction analysis (XRD)

XRD pattern of the CaONPs, Figure (4), showed crystalline phases with cubic structure according to Card No ICDD 00-037-1497. In Figure (4), the XRD peaks of the CaONPs are shown. The peaks at 32.3, 37.4, 54, 64.2, 67.5, 79.8, 88.5, and 91.4 correspond to the (111), (200), (220), (311), (222), (400), (331), and (420), respectively. These findings confirm the formation of a well-defined cubic crystal structure in the synthesized CaONPs.

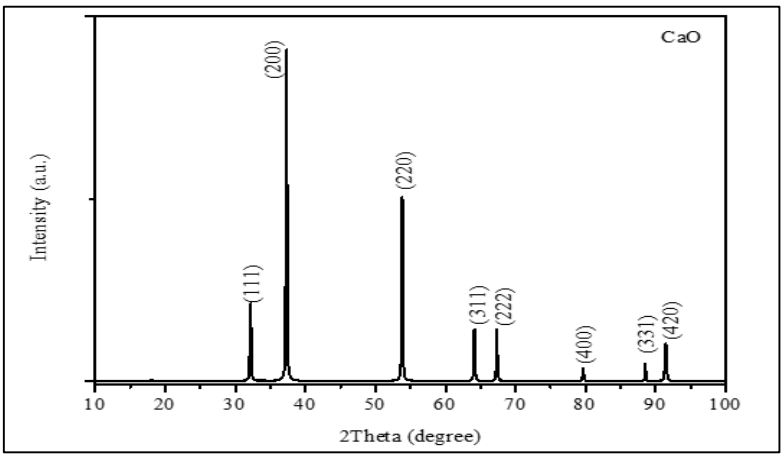

Figure (4): XRD OF CaO nanoparticles.

Field Emission Scanning Electron Microscopy (FE-SEM):

FE-SEM images, CaONPs were as about spherical nanoparticles with a size between 84.8 -163 nm, as shown in Figure(5). Recognizing that these particles contain fragments of diverse sizes and shapes.

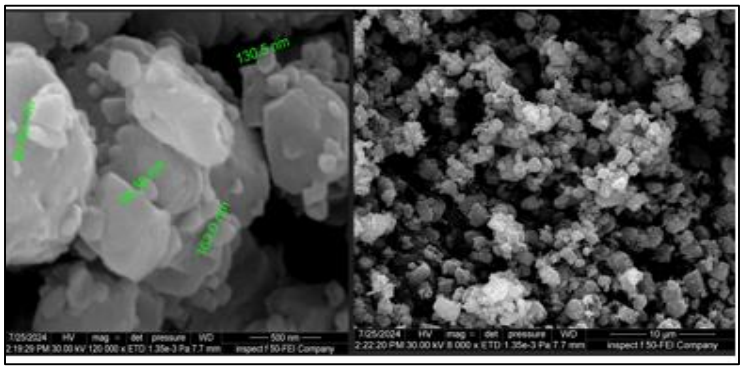

Figure (5): FE-SEM of the prepared CONPs.

Transmission Electron Microscopy (TEM)

TEM was employed to enhance the accuracy of our examination, as shown in Figure (6a). TEM image of the synthesized CaONPs revealed a particle size distribution ranging from 2 - 23 nm, with an average size estimated at 8 nm. This observation highlights the presence of quantum dots within the prepared nanoparticles and the previously mentioned nanosheets, as demonstrated in Figures (6a, b). Simultaneously, the mix of CaONPs and NAR produced a random network with a clear prominence of naringin-containing areas (dark areas), where the average particle size was about 20 nm, with the largest size being observed for the dark areas, which can be inferred to be naringenin-containing CaONPs Figure 6c, d.

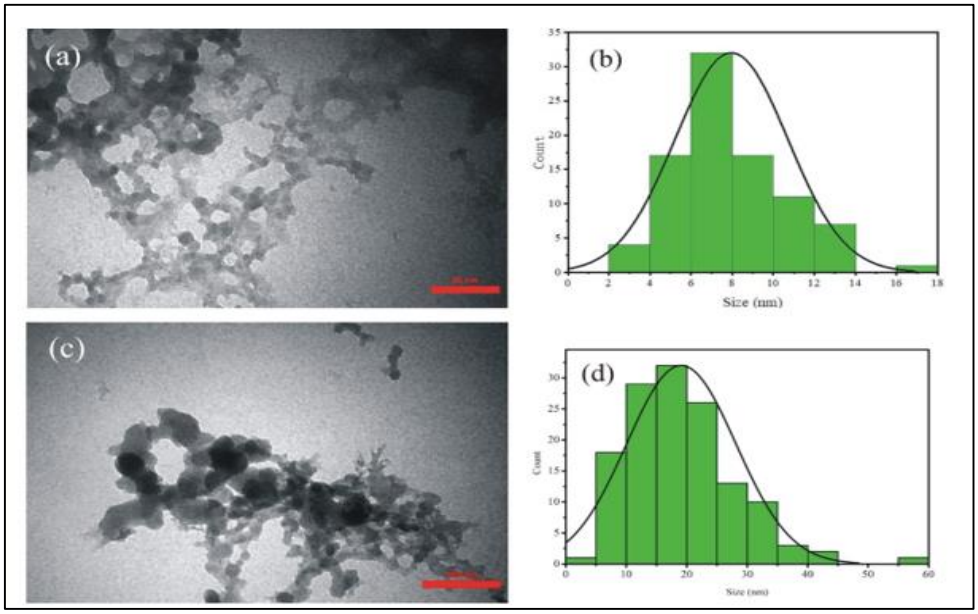

Figure (6): TEM of (a) the prepared CaONPs, (b) Size distribution of the prepared CaONPs TEM of (c) the prepared CaONPs-NAR (d): Size distribution of the prepared CaONPs-NAR

Effect of CaONPs and Naringenin Synthesized on *Staphylococcus aureus*

Figure (7) shows an increase in the size of the inhibition diameter around the hole of the comping CaONPs-NAR, and statistical analysis showed a significantly enhanced antibacterial activity against *S. aureus*.

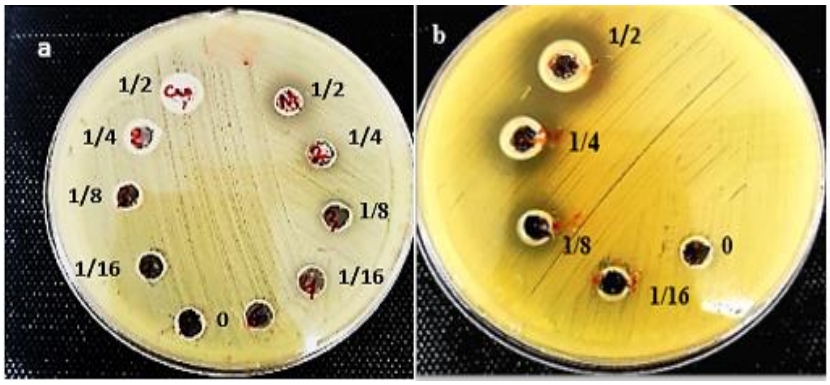

Figure (7): a: Zone inhibition of serial dilution CaONPs and Naringenin b: Zone inhibition of serial dilution CaONPs-Naringenin.

The maximum activity of CaONPs was with an average inhibition diameter of 10 ± 0.67 mm. The highest activity for Naringenin with an average inhibition diameter of (10 ± 0.33 mm), while CaONPs-NAR showed the best antibacterial results of 18 ± 0.67 Table 2. The statistical analysis of the ANOVA showed that the effect of the two substances on bacterial growth was highly significant ***(P≤ 0.001), which means that the effects observed are not due to random variation or chance Figure(8).

Table (2): Determinations of zone inhibition (mm) of prepared material against *S. aureus*.

S. aureus isolates	Zone inhibition of CaO NPs (mm)	Zone inhibition of NAR (mm)	Zone inhibition of CaO NPs-NAR (mm)
S2	10	10	19
S3	12	10	20
S4	10	11	17
Mean	10.67	10.33	18.67

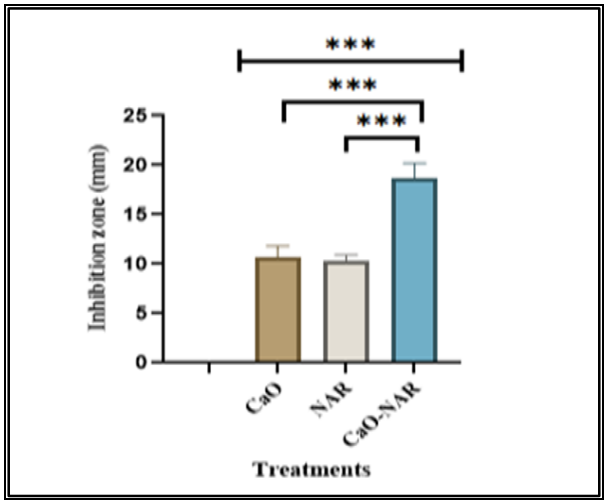

Figure (8): **Mean inhibition zone (mm) of prepared treatments against S. *aureus* isolates.**

CaONPs vs CaONPs-NAR (*P)**
NAR Vs CaONPs-NAR (* **P)

After confirming the antimicrobial activity of CaONPs, NAR, and CaONPs-NAR, the broth dilution method was used to determine the MIC and sub-MIC concentrations of CaONPs, NAR, and CaONPs-NAR to study their effect on

the expression of *lukE/D* genes in *S. aureus* isolates. MIC of all the treatments was scrutinized, and subMIC of CaONPs, Naringenin, and CaONPs-NAR was observed to be 1 /8, 1/ 4, and 1/16 mg/mL, respectively, against three replicates of *S. aureus*. The expression level of the *lukE* and *lukD* genes was assessed by real-time PCR, and the results (fold changes) were obtained using the 2−ΔΔCt comparative method. The gene expression is quantified for each sample, and the CT results for each sample are compared with the CT results for gene expression of the *SrRNA 16* (reference gene). Gene expression results showed decreased expression under the influence of different treatments, Tables 3 and 4. When NAR was used, a 73.1% and 67.1% reduction in *lukE* and *lukD* gene expression, respectively. In contrast, the effect of the CaONPs was used, resulting in a decrease of 91.17% and 95.5%. However, a 94.5% and 92.6% reduction were observed in gene expression when the two substances were combined. indicated a strong effect on the expression mechanisms in the bacteria.

Table (3): Gene expression values for the *lukE* gene and the reference gene *S. aureus* isolates under the effect of CaONPs, NAR, and CaONPs-NAR.

Sample	*SrRNA 16*	*luK E*	dct	ddct	Folding
Control 2	12.44	16.01	3.57	0.00	1.000
NAR	16.04	20.87	4.83	1.26	0.417
CaONPs	24.73	33.32	8.59	5.03	0.031
CaONPs-NAR	17.43	24.53	7.10	3.53	0.087
Control 3	9.15	14.88	5.73	0.00	1.000
NAR	16.12	23.75	7.63	1.90	0.268
CaONPs	20.13	28.60	8.47	2.74	0.150
CaONPs-NAR	7.34	22.15	14.81	9.08	0.002
Control 4	11.98	15.56	3.58	0.00	1.000
NAR	19.21	25.83	6.62	3.04	0.122
CaONPs	22.92	30.08	7.16	3.58	0.084
CaONPs-NAR	17.76	25.06	7.30	3.72	0.076

Table (4): Gene expression values for the *lukD* gene and the reference gene *S. aureus* isolates under the effect of CaONPs, NAR, and CaONPs-NAR.

Sample	*16SrRNA*	*luK D*	dct	ddct	Folding
Control 2	12.44	16.07	3.63	0.00	1.000
NAR	16.04	20.65	4.61	0.99	0.505
CONPs	24.73	38.39	13.66	10.04	0.001
CONPs-NAR	17.43	23.97	6.54	2.91	0.133
Control 3	9.15	15.26	6.10	0.00	1.000
NAR	16.12	23.69	7.57	1.46	0.363
CaONPs	20.13	30.31	10.18	4.07	0.059
CaONPs-NAR	7.34	22.48	15.14	9.03	0.002
Control 4	11.98	15.01	3.03	0.00	1.000
NAR	19.21	25.32	6.11	3.08	0.119
CONPs	22.92	29.72	6.80	3.77	0.074
CONPs-NAR	17.76	24.34	6.58	3.54	0.086

Analysis of variance (ANOVA) showed statistically significant differences between treatments at **** ($P \leq 0.0001$), indicating statistically significant differences between the means. CaONPs-NAR was the most effective in reducing gene expression levels, showing a stronger effect than NAR (Figure 9). The use of CaONPs-NAR significantly enhanced the efficacy of NAR, resulting in more potent inhibition of bacterial growth and greater reduction in gene expression of Lukocidin ED toxin. This could mean that the combined substance may affect additional growth mechanisms or have multiplying effects on cellular processes.

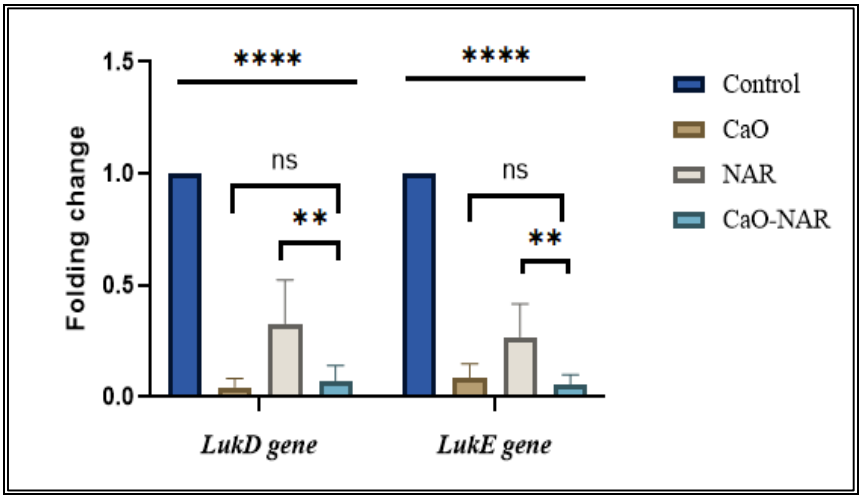

Figure (9): Fold of gene expression of *luk E/D* in three replicates of *S. aureus* with CaONPs, NAR, and CaONPs-NAR. Control vs CaONPs, NAR, CaONPs-NAR (**P), CaONPs vs CaONPs-NAR (ns), NAR Vs CaONPs-NAR (**P).**

The ability of CaONPs to significantly enhance the antibacterial efficacy of bioactive naringenin against multidrug-resistant (MDR) *S. aureus* has been demonstrated. The synergistic effect between CaONPs and NAR suggests a dual mechanism of action: physical disruption of the bacterial cell membrane by the nanoparticles, followed by increased intracellular access and bioactivity of NAR. This synergistic interaction is consistent with previous findings published in scientific literature. Yeh *et al*. (34) demonstrated that metallic nanoparticles can induce microscopic lesions in bacterial membranes, facilitating the penetration of therapeutic molecules. Similarly, the increased activity of NAR when delivered via nanocarriers has implications for both antibacterial and anticancer applications(35, 36).

Mechanistically, CaONPs are likely to compromise the integrity of the bacterial cell wall through oxidative stress or direct physicochemical interactions, such as electrostatic binding or lipid peroxidation. These changes reduce the structural resistance of the bacterial envelope, allowing more efficient passage of the bioactive compound. Once inside the cell, the natural compound, known to target bacterial enzymes or genetic material, can exert its effects more effectively, resulting in higher antibacterial outcomes. The reduction in the minimum inhibitory concentration

(MIC) observed in our study is consistent with that reported by Iram *et al*. (37), who found that CaONPs reduced the MIC of vancomycin against resistant enterococci by 50%. Additionally, the improvements in drug solubility and bioavailability observed when CaONPs were combined with sulfamethoxazole (38) further demonstrate the potential of nanoparticle-assisted delivery systems to overcome the solubility limitations of hydrophobic drugs.

Khan *et al*. also reported that the use of silver nanoparticles (AgNPs) with CaONPs demonstrated significant efficacy against methicillin-resistant *S. aureus* (MRSA) at concentrations ranging from 25–150 µg/ml, along with their ability to inhibit biofilm formation. The study also demonstrated that the compound maintained its antibacterial activity while reducing its toxicity to mammalian cells(39). In a study by Cristián *et al*., it was shown that CaONPs surface-modified with oleic acid and 25 nm in size achieved the highest reduction in *Escherichia coli* cell count, reaching 99.99% (40). In another study, Ikram *et al*. reported that CaONPs supplemented with 4% aluminum and starch resulted in an inhibition zone of 10.25 mm against *S. aureus* and 4.95 mm against *E. coli*, demonstrating the high efficacy of the composite particles (41).

Despite the promising results, some limitations must be acknowledged. This study was conducted in vitro, and while the results are encouraging, further in vivo studies are necessary to evaluate the pharmacokinetics, biodistribution, and long-term biocompatibility.

Overall, the results suggest that CaONPs, when combined with Naringenin, represent a promising and versatile platform for the development of next-generation antimicrobial therapeutics. These approaches could be particularly valuable in combating infections caused by multidrug-resistant pathogens, where traditional antibiotics alone are no longer effective.

Conclusion

The effect of calcium nanoparticle (CaONPs) or naringenin (NAR) may be limited when used alone, but their effect can be significantly enhanced when combined. Natural materials may help improve the distribution of calcium monophosphates on surfaces or in the medium, increasing their antibacterial efficacy. The interaction between CaONPs and bacteria can have different effects depending on the bacterial species and the properties of the material. Using naringin synergistically with nanoparticles also makes it more stable and effective as an antibacterial agent than when used alone. Interactions between different materials can lead to different outcomes in gene expression and bacterial response, with some formulations being more effective at killing bacteria, while others require a greater gene response.

References

1. Zainulabdeen, S. M. and Dakl, A. A. A. (2021). Pathogenicity and virulence factors in *Staphylococcus aureus*. *MJPS*, *8*(52113), 2.
2. Cheung, G. Y.; Bae, J. S. and Otto, M. (2021). Pathogenicity and virulence of *Staphylococcus* aureus. Virulence, 12(1), 547-569.
3. Ahmad-Mansour, N.; Loubet, P.; Pouget, C.; Dunyach-Remy, C.; Sotto, A.; Lavigne, J. P., *et al*. (2021). Staphylococcus aureus toxins: an update on their pathogenic properties and potential treatments. Toxins, 13(10), 677.
4. Oliveira, D.; Borges, A. and Simões, M. (2018). Staphylococcus aureus toxins and

their molecular activity in infectious diseases. Toxins, 10(6), 252.
5. Reyes-Robles, T.; Lubkin, A.; Alonzo III, F.; Lacy, D. B. and Torres, V. J. (2016). Exploiting dominant-negative toxins to combat Staphylococcus aureus pathogenesis. EMBO reports, 17(3), 428-440.
6. Abdel-hamed, A. H. A.; Abdel-Rhman, S. H. and El-Sokkary, M. A. (2016). Studies on leukocidins toxins and antimicrobial resistance in Staphylococcus aureus isolated from various clinical sources. African Journal of Microbiology Research, 10(17), 591-599.
7. Ghaffar, N.; Javad, S.; Farrukh, M. A.; Shah, A. A.; Gatasheh, M. K.; Al-Munqedhi, B. M., *et al*. (2022). Metal nanoparticles assisted revival of Streptomycin against MDRS Staphylococcus aureus. PLoS One, 17(3), e0264588.
8. Rasheed, N. A. and Hussein, N. R. (2021). Staphylococcus aureus: an overview of discovery, characteristics, epidemiology, virulence factors and antimicrobial sensitivity. European Journal of Molecular & Clinical Medicine, 8(3), 1160-1183.
9. Nikolic, P. and Mudgil, P. (2023). The cell wall, cell membrane and virulence factors of Staphylococcus aureus and their role in antibiotic resistance. Microorganisms, 11(2), 259.
10. Nasir, G. A.; Khudhair, I. A.; Najm, M. A. and Mahmood, H. M. (2022). Nanotechnology at the molecular level. Al-Rafidain Journal of Medical Sciences (ISSN 2789-3219), 3, 71-74.
11. Loka, S.; Krishnan, S.N.; Anandan, J. and Shanmugam, R. (2024). Nanotechnology Perceptions ISSN 1660-6795 www (Internet), 20, Nanotechnology Perceptions.
12. Tang, Z. X.; Yu, Z.; Zhang, Z. L.; Zhang, X. Y.; Pan, Q. Q. and Shi, L. E. (2013). Sonication-assisted preparation of CaO nanoparticles for antibacterial agents. Química Nova, 36, 933-936.
13. Ramola, B.; Joshi, N. C.; Ramola, M.; Chhabra, J. and Singh, A. (2019). Green synthesis, characterisations and antimicrobial activities of CaO nanoparticles. Oriental Journal of Chemistry, 35(3), 1154–1157.
14. Turgut, B. A. and Bezirganoğlu, İ. (2022). Foliar application of CaO nanoparticles and salicylic acid on Medicago sativa seedlings enhances tolerance against Fusarium oxysporum. Physiological and Molecular Plant Pathology, 122, 101926.
15. Abbas, I. K. and Aadim, K. A. (2022). Synthesis and study of structural properties of calcium oxide nanoparticles produced by laser-induced plasma and its effect on antibacterial activity. Science and Technology Indonesia, 7(4), 427-434.
16. Yazicilar, B.; Nadaroğlu, H.; Alayli, A.; Nadar, M.; Gedikli, S. and Bezirğanoğlu, I. (2024). Mitigation of drought stress effects on alfalfa (Medicago sativa L.) callus through CaO nanoparticles and graphene oxide in tissue culture conditions. Plant Cell, Tissue and Organ Culture (PCTOC), 157(3), 54.
17. Duda-Madej, A.; Stecko, J.; Sobieraj, J.; Szymańska, N. and Kozłowska, J. (2022). Naringenin and its derivatives-Health-promoting phytobiotic against resistant bacteria and fungi in humans. Antibiotics, 11(11), 1628.
18. Podder, B.; Song, H. Y. and Kim, Y. S. (2014). Naringenin exerts cytoprotective effect against paraquat-induced toxicity in human bronchial epithelial BEAS-2B cells through NRF2 activation. Journal of microbiology and biotechnology, 24(5), 605-613.
19. Song, H. S.; Bhatia, S. K.; Gurav, R.; Choi, T. R.; Kim, H. J.; Park, Y. L., *et al.* (2020). Naringenin as an antibacterial reagent controlling of biofilm formation and fatty acid metabolism in MRSA. BioRxiv, 2020-03.
20. Wang, L. H.; Wang, M. S.; Zeng, X. A.; Xu, X. M. and Brennan, C. S. (2017). Membrane and genomic DNA dual-targeting of citrus flavonoid naringenin against Staphylococcus aureus. Integrative Biology, 9(10), 820-829.
21. Sheng, Q.; Hou, X.; Wang, Y.; Wang, N.; Deng, X.; Wen, Z., *et al.*. (2022). Naringenin microsphere as a novel adjuvant reverses colistin resistance via various strategies against multidrug-resistant Klebsiella pneumoniae infection. Journal of Agricultural and Food Chemistry, 70(51), 16201-16217.

22. Firrman, J.; Liu, L.; Argoty, G. A.; Zhang, L.; Tomasula, P.; Wang, M., *et al*. (2018). Analysis of temporal changes in growth and gene expression for commensal gut microbes in response to the polyphenol naringenin. Microbiology insights, 11, 1178636118775100.
23. Atshan, S. S.; Shamsudin, M. N.; Karunanidhi, A.; van Belkum, A.; Lung, L. T. T.; Sekawi, Z., *et al.* (2013). Quantitative PCR analysis of genes expressed during biofilm development of methicillin resistant *Staphylococcus aureus* (MRSA). Infection, genetics and evolution, 18, 106-112.
24. Elbargisy, R. M. (2022). Distribution of leukocidins, exfoliative toxins, and selected resistance genes among methicillin-resistant and methicillin-sensitive Staphylococcus aureus clinical strains in Egypt. The Open Microbiology Journal, 16(1).
25. Adaikalam, K.; Hussain, S.; Anbu, P.; Rajaram, A.; Sivanesan, I. and Kim, H. S. (2024). Eco-friendly facile conversion of waste eggshells into CaO nanoparticles for environmental applications. Nanomaterials, 14(20), 1620.
26. Ng'uni, T.; Mothlalamme, T.; Daniels, R.; Klaasen, J. and Fielding, B. C. (2015). Additive antibacterial activity of naringenin and antibiotic combinations against multidrug resistant *Staphylococcus aureus*.
27. do Amparo Madureira, J.; Marinho, B. M.; Carvalho, S. M.; de Fátima Leite, M. and Borsagli, F. G. M. (2024). Sustainable calcium oxide nanoparticles based on agroindustry waste for potential endodontics applications. Materials Chemistry and Physics, 320, 129426.
28. Fawzi, F. H. (2025). Antimicrobial Activity of Biosynthesized Selenium Nanoparticles from Staphylococcus warneri and its Impact on the PhzM Gene Expression in Clinical *Pseudomonas aeruginosa* Isolates. Iraqi journal of biotechnology, 24(1).
29. Abbas AL-Essawi, I. and Mahmood, H. M. (2024). Effect of Gold Nanoparticles on hmgA Gene Expression of Pseudomonas aeruginosa Isolates. Journal of Nanostructures, 14(4), 1030-1040.
30. Al-Mathkhury, H. J. F. (2025). Estimation the Expression of Glucose-Dependent Biofilm-Encoding icaA and icaD Genes in Methicillin Resistant *Staphylococcus aureus* Isolates. Iraqi journal of biotechnology, 24(1).
31. Betelhem, T.; Shubisa, A. L. and Bari, F. D. (2022). Isolation, identification and antimicrobial resistance of Staphylococcus aureus isolates from mastitis cases of lactating dairy cows found in Sululta and Holleta Towns, Oromia, Ethiopia. Agrobiological Records, 8, 27-34.
32. Yaseen, A. F. and Al-Draghi, W. A. (2025). Investigate Prevalence of (blaIMP, blaOXA-40, and blaGES) Genes in Carbapenems Resistance Pseudomonas aeruginosa Isolates. Iraqi journal of biotechnology, 24(1).
33. Chen, L.; Tang, Z. Y.; Cui, S. Y.; Ma, Z. B.; Deng, H.; Kong, W. L., *et al.* (2020). Biofilm production ability, virulence and antimicrobial resistance genes in *Staphylococcus aureus* from various veterinary hospitals. Pathogens, 9(4), 264.
34. Yeh, Y. C.; Huang, T. H.; Yang, S. C.; Chen, C. C. and Fang, J. Y. (2020). Nano-based drug delivery or targeting to eradicate bacteria for infection mitigation: a review of recent advances. Frontiers in chemistry, 8, 286.
35. Motallebi, M.; Bhia, M.; Rajani, H. F.; Bhia, I.; Tabarraei, H.; Mohammadkhani, N., *et al.* (2022). Naringenin: A potential flavonoid phytochemical for cancer therapy. Life Sciences, 305, 120752.
36. Pachaiappan, R.; Rajendran, S.; Show, P. L.; Manavalan, K. and Naushad, M. (2021). Metal/metal oxide nanocomposites for bactericidal effect: A review. Chemosphere, 272, 128607.
37. Iram, S.; Khan, J. A.; Aman, N.; Nadhman, A.; Zulfiqar, Z. and Yameen, M. A. (2016). Enhancing the anti-enterococci activity of different antibiotics by combining with metal oxide nanoparticles. Jundishapur Journal of Microbiology, 9(3), e31302.
38. Jayaraj, S.; Jayasree, J. N. and Murali, T. (2024). Applications and synthesis processes of biosynthesized calcium oxide nanoparticles with sulfamethoxazole: a comprehensive review. Nano-Structures & Nano-Objects, 39, 101244.
39. Khan, M. I.; Mazumdar, A.; Pathak, S.; Paul, P.; Behera, S. K.; Tamhankar, A. J., *et*

al. (2020). Biogenic Ag/CaO nanocomposites kill Staphylococcus aureus with reduced toxicity towards mammalian cells. Colloids and Surfaces B: Biointerfaces, 189, 110846.

40. Silva, C.; Bobillier, F.; Canales, D.; Antonella Sepúlveda, F.; Cament, A.; Amigo, N., *et al.* (2020). Mechanical and antimicrobial polyethylene composites with CaO nanoparticles. Polymers, 12(9), 2132.
41. Ikram, M.; Haider, A.; Bibi, S. T.; Ul-Hamid, A.; Haider, J.; Shahzadi, I., *et al.* (2022). Synthesis of Al/starch co-doped in CaO nanoparticles for enhanced catalytic and antimicrobial activities: experimental and DFT approaches. RSC advances, 12(50), 32142-32155.